coatings

MDPI

Article

Research on Titanium Ion Etching Pretreatment Process on Cemented Carbide Before DLC Film Deposition

Chao Li [1], Juan Chen [1,*] and Lei Huang [2]

[1] School of Mechanical Engineering, Nantong University, str. Seyuan Road 9, Nantong 226019, China; mclee@ntu.edu.cn
[2] School of Mechanical Engineering, Nanjing University of Science and Technology, str. Xiaolingwei 200, Nanjing 210094, China; huanglei_0826@njust.edu.cn
* Correspondence: chenjuanwhy@ntu.edu.cn

Abstract: Before depositing a thin film, modifying the substrate surface was a crucial step in the film preparation process, having a decisive impact on the final properties of the film. In addition to additive methods such as preparing transition layers, subtractive methods such as etching treatment could also enhance the performance of the film. Using titanium ions to etch and pretreat the surface of cemented carbide was an effective optimization method for depositing DLC films. This paper investigated the influence of process parameters for titanium ion etching of cemented carbide on the substrate surface. By varying the substrate negative bias voltage, medium-frequency current, and argon gas flow rate, the etching rate, roughness, and elemental changes of the etched surface were studied. DLC films were then deposited on the etched surfaces to investigate the effect of the changes of surface characteristics on subsequent film deposition. The research revealed that the substrate negative bias voltage had the most significant impact on the etching rate, while the MF current affected the surface roughness. The increase in surface roughness can enhance the deposition rate. The changes in C/W ratio did not exhibit a clear impact pattern on the DLC film. However, an increase in Co element content improved the properties of the DLC film due to the diffusion of sub-surface Co element.

Keywords: surface pre-treatment; Ti ion etching treatment; film deposition; cemented carbide

check for updates

Academic Editor: Torsten Brezesinski

Received: 9 March 2025
Revised: 31 March 2025
Accepted: 3 April 2025
Published: 7 April 2025

Citation: Li, C.; Chen, J.; Huang, L. Research on Titanium Ion Etching Pretreatment Process on Cemented Carbide Before DLC Film Deposition. *Coatings* **2025**, *15*, 434. https://doi.org/10.3390/coatings15040434

Copyright: © 2025 by the authors. Licensee MDPI, Basel, Switzerland. This article is an open access article distributed under the terms and conditions of the Creative Commons Attribution (CC BY) license (https://creativecommons.org/licenses/by/4.0/).

1. Introduction

Diamond-like carbon (DLC) films are thin film materials that have been widely studied in recent years. Because of their high hardness and wear resistance, DLC films have very broad application prospects in fields such as cutting tools, medical instruments, robotics, and molds [1,2]. However, the significant drawbacks of DLC films, such as their instability, tendency to graphitize, and poor adhesion, greatly limit their applications. At present, the properties of DLC films have been significantly improved through methods like adjusting the preparation process, introducing doping elements, establishing gradient structures, and constructing composite multilayer films. Among these, pre-treating the substrate surface to alter its characteristics is also an effective way to enhance the performance of DLC films [3,4]. Appropriately increasing the surface roughness of the substrate can provide more nucleation sites for carbon atoms, thereby increasing the deposition rate. The mechanical interlocking effect brought about by roughness helps to enhance the adhesion strength between the film and the substrate [5,6]. Enhancing the chemical activity of the substrate surface or modifying the elemental distribution on the substrate surface can

facilitate bonding between carbon atoms and substrate elements, which is conducive to improving the film–substrate adhesion strength [4,7,8].

Magnetron sputtering is one of the most commonly used methods of DLC film preparation in recent decades. It is not only used for film deposition, but also for surface treatment. For film deposition, deposition particles are ionized and excited from the solid or gaseous state and finally deposited on the substrate surface to form a thin film. Among several types of magnetron sputtering technologies, the ionization rate of particles is very low in both direct-current (DC) and medium-frequency (MF) magnetron sputtering, whereas high-power pulsed magnetron sputtering can significantly increase the ionization rate. When the particles are deposited on the substrate surface, since they carry a certain amount of energy, some of them will embed into the substrate after releasing energy, while others will be detached due to collisions [9–12]. These two phenomena are the deposition phenomenon and the sputtering phenomenon on the substrate surface in magnetron sputtering coating. Thin film preparation is the competitive result of these two phenomena. For thin film deposition, appropriately increasing the energy of the particles helps the particles achieve sub-surface injection, which has a positive impact on improving the adhesion strength [13–15]. However, if the particle energy is too high, when the particles bombard the substrate strongly, the released energy will take away the deposited particles and some atoms on the substrate surface [16–18]. At this time, the sputtering process completely suppresses the deposition process, and the thin film cannot be formed. Instead, it will have an etching effect on the substrate, and the adsorbates, oxides on the substrate surface, and even the material of the substrate itself will be etched and detached. The process is no longer film deposition, but surface etching treatment.

The etching method is often used in the vacuum chamber before coating to clean the substrate surface with argon glow discharge. The etching effect of argon is very slight, which can remove the oxides on the substrate surface while ensuring that the surface morphology of the substrate does not change significantly [19,20]. Oxygen and hydrogen are also commonly used gases for surface etching, which use chemical reactions to remove organic substances and oxides on the substrate surface, respectively [21]. After cleaning, the chemical activity of the substrate surface is higher, which is favorable for improving the performance of subsequently deposited films. These gases themselves will not form films, so they can be used for etching treatment. However, the etching effect of gas ions on the substrate surface is limited, and the change in substrate properties is minimal.

If metal ions are used to etch the substrate, the properties of the substrate can be significantly altered. Although it is extremely easy for metal ions to form films, if they also have high energy, the sputtering phenomenon of metal ions can also suppress the deposition phenomenon to form an etching effect. In Fu's research, W element was used to etch the substrate, and a DLC film with better performance was obtained [22]. High-power pulsed magnetron sputtering (HiPIMS) technology has a high ionization rate for metals. It can produce a large number of high-energy metal ions to etch the substrate to construct a metal transition zone with high roughness. This metal transition zone can improve the stress distribution at the film–substrate interface, thereby enhancing the adhesion strength of DLC films. The surface etched by Cr element using HiPIMS technology has been proven to effectively improve the adhesion strength and load-bearing capacity of DLC films and delay the delamination and deformation of the films [23,24]. Cathodic arc evaporation can provide etching metal ions as well. The increase in the surface roughness of an etched surface has an inhibitory effect on the propagation of lateral cracks in TiAlN film [25].

In previous studies, it has been proven feasible to use MF magnetron sputtering to achieve etching treatment of cemented carbide with Ti ions. Unlike in other methods, due to the low ionization rate of MF magnetron sputtering, the concentration of Ti ions

is very low. After completing the etching of the substrate, the energy-depleted Ti ions will be dislodged from the substrate due to the bombardment of subsequent ions and cannot form a metal layer [26]. Based on this, this paper conducted a more in-depth study of Ti ion etching treatment by MF magnetron sputtering. Single-factor experiments on substrate negative bias, medium-frequency current, and argon flow rate were conducted to investigate the changes in the morphology and elemental distribution of the substrate surface. Additionally, the impact of these changes in substrate surface characteristics on the properties of Ti-DLC films was further investigated.

2. Experiment Details

2.1. Etching Pre-Treatment and DLC Films Deposition

The MC-Hybrid coating system, equipped with a pair of rectangular titanium targets, was utilized for both the Ti ion etching treatment and the deposition of DLC films. The Ti ion etching process was executed using the mid-frequency magnetron sputtering technique, where the Ti targets generated the required Ti ion. The titanium targets were rectangular targets, each with a length of 300 mm, a width of 72 mm, and a thickness of 5 mm. Meanwhile, the DLC films were prepared by mid-frequency magnetron sputtering, but with a 99.999% purity ethyne rectangular target serving as the carbon source. Cemented carbide YG8 was chosen as the substrate material.

Prior to the deposition process, the YG8 samples underwent polishing and cleaning using an ultrasonic cleaner. The Ti ion etching treatment lasted for 40 min. During the etching process, the MF magnetron sputtering current was set to 4.0 A, with a power density of 10.3 W/cm^2 and a current density of 18 mA/cm^2. A pulse DC negative bias voltage of −1200 V was applied to the substrates. The argon flow rate was maintained at 80 sccm, and the chamber pressure was kept at 1.2 Pa. When used as variables, the range of the substrate negative bias was −1000 V to −1400 V, the range of the MF current was 3.0 A to 5.0 A, and the range of the argon flow rate was 80 sccm to 140 sccm. For the MF current ranging from 3.0 A to 5.0 A, the corresponding power densities were 7.5, 8.8, 10.3, 11.8, and 13.3 W/cm^2, respectively.

Following the etching treatment, Ti-DLC films were deposited onto the etched surfaces. During the film deposition process, the current was adjusted to 4.0 A, with a bias voltage of −1000 V applied for 40 min. The argon and ethyne flow rates were set to 100 sccm and 20 sccm, respectively, while the chamber pressure was maintained at 1.4 Pa. The chamber temperature was held at 100 °C throughout both the etching treatment and the DLC deposition process.

2.2. Characteristics Measurement

The etching depth was obtained by measuring the step height between the etched surface and the original surface using a stylus profiler (Dektak XT by Bruker). The composition and bonding of elements were analyzed using Energy Dispersive Spectrometry (EDS, Oxford). The carbon structure of the DLC film was characterized by a micro-Raman spectrometer (Renishaw inVia). The laser radiation wavelength of the Raman spectroscopy used was 514 nm. The adhesion strength was assessed using a coating adhesion scratch tester (WS−2005), with the scratch morphology visualized under a metallographic microscope. Tribological properties were evaluated on a reciprocating ball-on-disk tribometer (UMT-2 by Bruker), which automatically recorded the friction coefficient. The friction tests involved Ti6Al4V balls under dry friction conditions, conducted at 25 °C and 30% relative humidity. These tests maintained a constant load of 3 N, a velocity of 8 mm/s, and a duration of 30 min. The wear rates of the DLC films were calculated based on cross-sectional profiles of the wear tracks obtained.

3. Results and Discussion

3.1. Surface Characteristics Changed by Etching Parameters

3.1.1. Substrate Bias Voltage

The study on the impact of substrate negative bias voltage during etching treatment was conducted to investigate its effect on etch depth and surface morphology. The variations in etch depth and surface roughness were illustrated in Figure 1. As the bias voltage increased from −1000 V to −1400 V, the etch depth increased from 363 nm to 750 nm, with a continuous improvement in etch rate. The surface roughness reached its lowest point at −1100 V, at 35.62 nm, and peaked at −1300 V, at 43.20 nm.

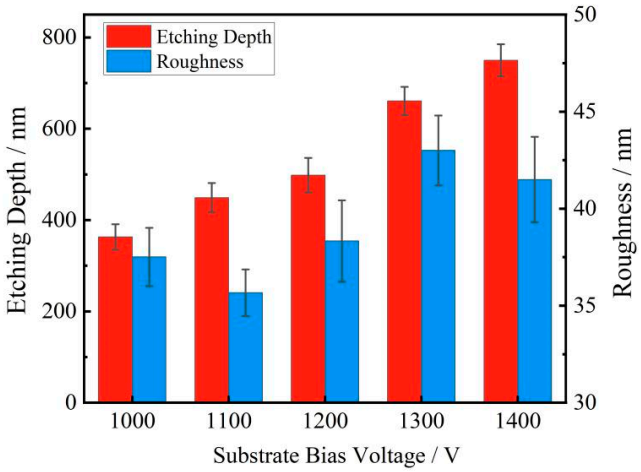


Figure 1. Etch depth and surface roughness changing with bias voltages.

From the three-dimensional morphology diagram of the etched surface (Figure 2), it was observed that the sample etched at a bias voltage of −1100 V exhibited the lowest roughness, with a smooth surface and sparsely distributed undulations, indicating good surface quality. The sample etched at −1300 V had more prominent protrusions on its surface, with sizes close to those of WC grains, which could be attributed to the exposure of grains. The scale of surface concavities and convexities decreased, showing a trend of being small and dense. Changes in the three-dimensional morphology suggested that between −1000 V and −1200 V, the energy of Ti ions was still relatively low, and the etching effect on the substrate surface mainly involved the removal of weakly bonded micromaterials, with limited damage to grains. When the bias voltage reached −1300 V, the energy of Ti ions increased to a higher level, marking the second stage of etching. At this stage, surface micromaterials were rapidly removed, exposing WC grains. Subsequently, the surface microelectric field gradually distorted, causing Ti ions to concentrate on damaging WC grains. After the grains were damaged, the microelectric field flattened out again, and the etching effect of Ti ions on the overall surface intensified once more. Therefore, a slight decrease in roughness was observed again at a bias voltage of −1400 V.

After EDS detection, the content of each element in the YG8 substrate is shown in Figure 3. After removing impurity phases and oxide phases, the atomic content of C, W, and Co were 53.22%, 34.43%, and 12.35%, respectively. The ratio of the atomic content of C to W elements was 1.55.

The elemental composition of the substrate surface shows significant changes after being treated with Ti ion etching. The chemical etching effect during the etching process had an obvious destructive impact on the WC grains. After the W-C bonds were broken, some C atoms bonded with Ti atoms and detached from the substrate. This resulted in a decrease in the proportion of C element. As a binder, Co can be easily removed due to

particle bombardment. The element content changing with the etching voltages is shown in Table 1. When the voltage is low, the C/W ratio only decreases slightly. This indicates that the energy of the etching particles is relatively low at this time, and their destructive effect on the WC grains is limited. However, once the voltage reaches 1300 V, the C/W ratio drops significantly. This demonstrates that the average energy of the Ti ions has reached a certain threshold at this stage, making their destructive effect on the W-C bonds much stronger. The content of Co element had decreased significantly compared with the substrate, but it showed an upward trend with the increase in voltage. There are two main reasons for this phenomenon: First, after the content of C decreased, in terms of the data, the content of other elements increased as a whole. The content of Co was stable compared with content of W element. Second, when the voltage was low, the energy of Ti ions had a limited destructive effect on WC grains, but it could easily remove Co element. As the etching of WC grains by Ti ions became more in-depth, the Co element in the sub-surface layer, which is not easy to remove directly, absorbed energy and diffused. This led to an increase in the content of Co element.

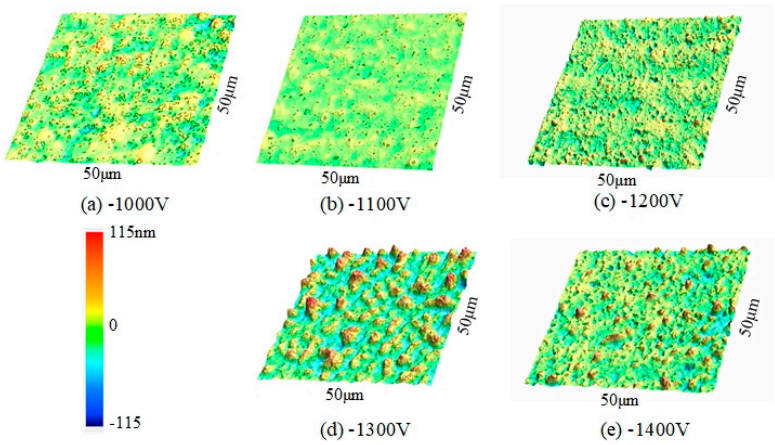


Figure 2. Three-dimensional morphology images of etched surfaces with bias voltages: (**a**) −1000 V; (**b**) −1100 V; (**c**) −1200 V; (**d**) −1300 V; (**e**) −1400.

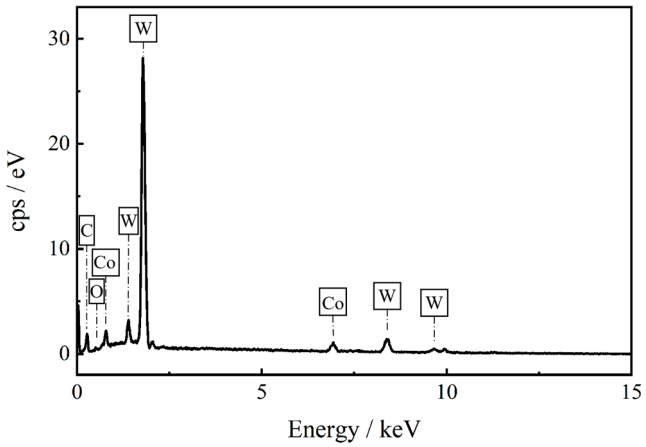


Figure 3. Element content of YG8.

Table 1. The element content of etched surfaces with bias voltages.

Substrate Bias Voltage/V	C at%	W at%	C/W Ratio	Co
1000	54.56	37.89	1.44	7.55
1100	54.05	38.33	1.41	7.62
1200	54.82	37.30	1.47	7.88
1300	48.33	43.16	1.12	8.51
1400	47.76	43.82	1.09	8.42

3.1.2. MF Current

As the MF current increased from 3.0 A to 5.0 A, the etching depth fluctuated from 383 nm to 449 nm and then decreased to 423 nm, as shown in Figure 4. The etching depth during the etching treatment exhibited a fluctuating trend with the increase in MF current, but the variation range was relatively small. The roughness rose from 19.25 nm to 39.00 nm as the MF current increased from 3.0 A to 4.0 A and then dropped back to 36.75 nm. As the MF current increased, the roughness generally increased and then tended to stabilize. This indicated that changes in the MF current had a minor impact on the etching depth but had a decisive influence on the surface roughness.

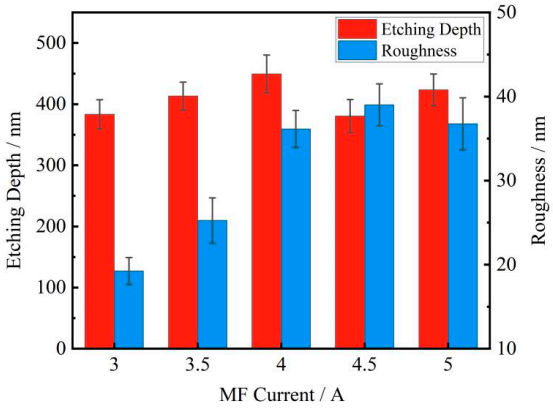


Figure 4. Etch depth and surface roughness changing with MF currents.

From the three-dimensional topography of the etched surfaces (Figure 5), it can be observed that as the MF current increased from 3.0 A to 4.0 A, the pits on the etched surface tended to become denser and deeper. Additionally, many sharp peaks appeared in the morphology of the 4.0 A sample, indicating that the WC grains on the surface began to gradually emerge at this point. For the 4.5 A sample, the density of peak-and-valley morphology on the surface decreased significantly, with fewer fine peaks and more prominent larger peaks. The pit morphology also decreased but showed obvious signs of merging. When the MF current for etching treatment increased to 5.0 A, the morphology of peaks and pits tended to become smoother and more evenly distributed.

The key impact of the changes in MF current on the etching treatment was reflected in the variation in Ti ions density. An increase in MF current enhanced the ionization rate of argon within the vacuum chamber, which, in turn, increased the density of argon ions sputtering the titanium target. This led to improved excitation efficiency of the titanium target, resulting in an increase in the density of Ti ions in the plasma. Since the argon ions ionized by the medium-frequency power supply were confined to the area on the target surface by the magnetic field, there was no increase in the argon ions bombarding the substrate surface. Although the density of etching particles increased with the rise in Ti ions, the energy of these particles did not change significantly, and the surface diffusion energy

remained roughly constant. Therefore, the etching depth did not increase accordingly. However, due to the increase in Ti ions, more Ti ions combined with the C on the substrate surface, exacerbating the destruction of WC grains on the surface. Consequently, an increase in roughness was observed.

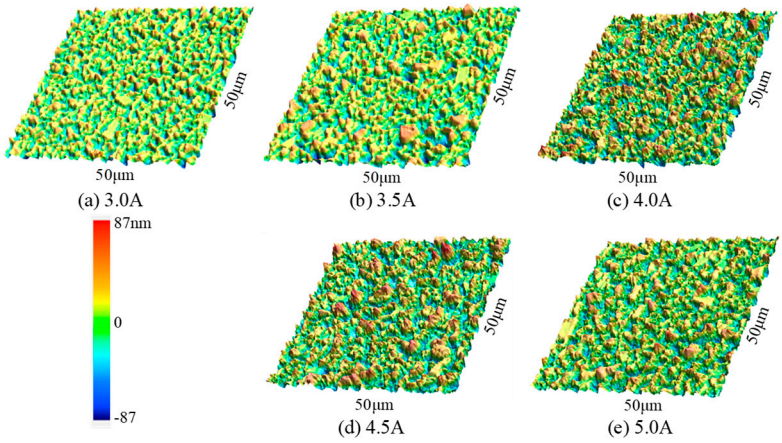


Figure 5. Three-dimensional morphology images of etched surfaces with MF currents: (**a**) 3.0 A; (**b**) 3.5 A; (**c**) 4.0 A; (**d**) 4.5 A; (**e**) 5.0 A.

The element content changing with the MF currents is shown in Table 2. When the medium-frequency current was 3.0 A, the C/W ratio on the etched surface was relatively high. This was because the power density was very low, resulting in both the density and energy of Ti ions being at low levels. When the medium-frequency current was increased from 3.5 A to 5.0 A, the change in the C/W ratio was minimal. The increase in power density did not significantly enhance the energy of Ti ions. The gradual increase in the content of Co element was due to the fact that Ti ions did not have sufficient energy to etch deeply into the WC grains and instead acted on the grain boundaries. The etching effect enlarged the surface voids, facilitating the diffusion of Co element.

Table 2. The element content of etched surfaces with MF currents.

Mf Current/A	C at%	W at%	C/W Ratio	Co
3	52.37	39.67	1.32	7.96
3.5	49.66	41.74	1.19	8.60
4	48.04	42.52	1.13	9.44
4.5	42.78	45.99	0.93	11.23
5	47.39	42.31	1.12	10.30

3.1.3. Ar Flow

As the Ar flow increased from 80 sccm to 140 sccm, the etching depth and surface roughness first decreased and then increased, as shown in Figure 6. The etching depth decreased from 449 nm to 375 nm and then increased to 464 nm. The roughness decreased from 36.14 nm to 34.3 nm and then increased to 41.33 nm. At lower Ar flow, the particle density in the vacuum chamber was low, which was conducive to increasing the atomic ionization rate. Increasing the Ar flow directly increased the number and density of plasma.

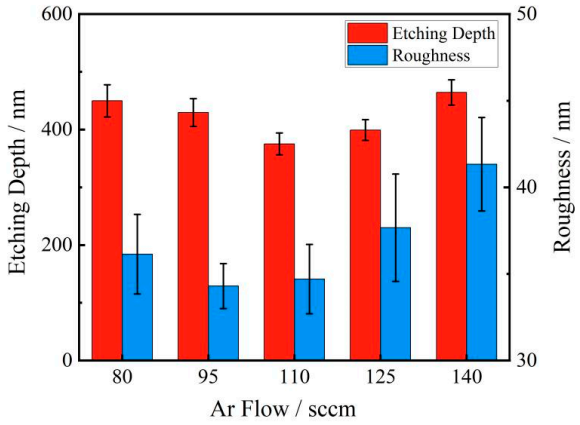


Figure 6. Etch depth and surface roughness changing with Ar flow.

Based on the three-dimensional topography of the etched surfaces, when the Ar flow increased from 80 sccm to 110 sccm, the surface morphology changed little, remaining relatively flat with evenly distributed peaks and valleys of small amplitudes. When the Ar flow rose to 125 sccm, the surface roughness increased significantly, with the peaks and valleys fully exposed. As the Ar flow further increased to 140 sccm, the peaks and valleys on the substrate surface became more prominent. Since argon ions are ionized near the target surface, changes in the overall Ar flow in the vacuum chamber have little impact on the process of argon ionization to produce argon ions. Therefore, the sputtering effect of argon ions on the titanium target does not change significantly with variations in the Ar flow. Some related studies suggested that an increase in Ar flow or gas pressure enhances the plasma density within the chamber, reducing the mean free path of deposited particles and decreasing the deposition rate [20,27]. Titanium ions inherently have low surface diffusion energy. When the Ar flow increases, particle collisions in the plasma intensify, further lowering the surface diffusion energy of titanium ions. Upon reaching the substrate surface, titanium ions lack sufficient energy to penetrate the sub-surface layer and form strong bonds with the substrate, instead remaining free on the surface. Therefore, the primary effect of titanium ions on the substrate surface is etching rather than nucleation and film formation. However, the impact of increased Ar flow on titanium ions is complex. Before reaching the substrate surface, an increase in Ar flow causes energy loss to titanium ions. When titanium ions are free on the substrate surface, they collide with more argon ions, and the energy exchange significantly boosts the surface diffusion energy of titanium ions. When the Ar flow exceeds 110 sccm, the increase in titanium ion diffusion energy on the substrate surface due to argon ions outweighs the energy loss caused by the reduced mean free path, exacerbating the damage to WC grains. Consequently, the surface roughness of the substrate increases significantly. When the Ar flow reaches 140 sccm, the proportion of collisions between argon ions and titanium ions on the substrate surface continues to rise. At this point, in addition to the direct etching of the substrate by argon ions and titanium ions, collisions between these two types of particles on the substrate surface produce secondary etching. In Figure 7e, when the Ar flow reaches 140 sccm, numerous fine textures appear on the exposed WC grains, demonstrating that ion collisions have caused significant secondary etching.

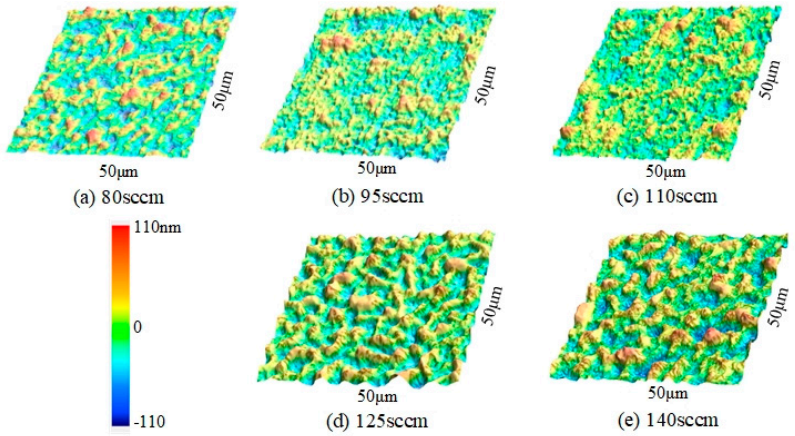


Figure 7. Three-dimensional morphology images of etched surfaces with Ar flow: (**a**) 80 sccm; (**b**) 95 sccm; (**c**) 110 sccm; (**d**) 125 sccm; (**e**) 140 sccm.

The element content changing with the Ar flows is shown in Table 3. From the trend of the C/W ratio, it can be seen that changing the Ar flow rate has a relatively small impact on the elemental distribution on the substrate surface. This indicates that the Ar flow rate has limited influence on the energy of Ti ions. The etching effect of Ti ions on the substrate in the vertical direction is relatively stable, which is consistent with the change in etching depth. However, the changes in the surface roughness of the substrate and the increase in Co element reflect that the increase in Ar flow rate mainly affects the etching process through the surface diffusion energy of Ti ions. Ti ions move in a direction parallel to the substrate surface, causing horizontal etching of the substrate surface morphology and enhancing the diffusion of Co elements.

Table 3. The element content of etched surfaces with Ar flow.

Ar Flow/sccm	C at%	W at%	C/W Ratio	Co
80	48.04	42.52	1.13	9.44
95	46.92	43.05	1.09	10.03
110	47.50	42.03	1.13	10.47
125	47.26	41.83	1.13	10.91
140	51.12	39.02	1.31	9.86

3.2. Key Factors of Etched Surface Influencing DLC Properties

3.2.1. Surface Roughness

After mirror polishing and cleaning, the surface roughness of the cemented carbide substrate can be reduced to below 5 nm. Following the Ti ion etching treatment, the surface roughness increased significantly to around 35 nm. The WC grains were partially destroyed and exposed. The gaps between the grains were enlarged as shown in Figure 8. After depositing a Ti-DLC film on the etched surface, the substrate surface morphology changed very little due to the thin film thickness of only about 1 μm.

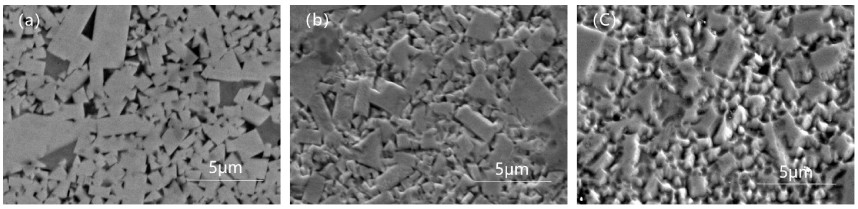


Figure 8. SEM images of surface morphology: (**a**) polished surface; (**b**) Ti ion etched surface; (**c**) Ti-DLC film surface.

The change in roughness is the most intuitive factor of the substrate surface change after etching treatment. The roughness of the etched surface has a strong correlation with the thickness of the Ti-DLC film according to Figure 9a. The thickness of the film increases with the increase in roughness. This is because a smooth surface is not conducive to the nucleation and growth of C atoms. A larger roughness can block the diffusion and migration of C atoms in the parallel direction after they reach the substrate surface. This results in a higher deposition rate of the film.

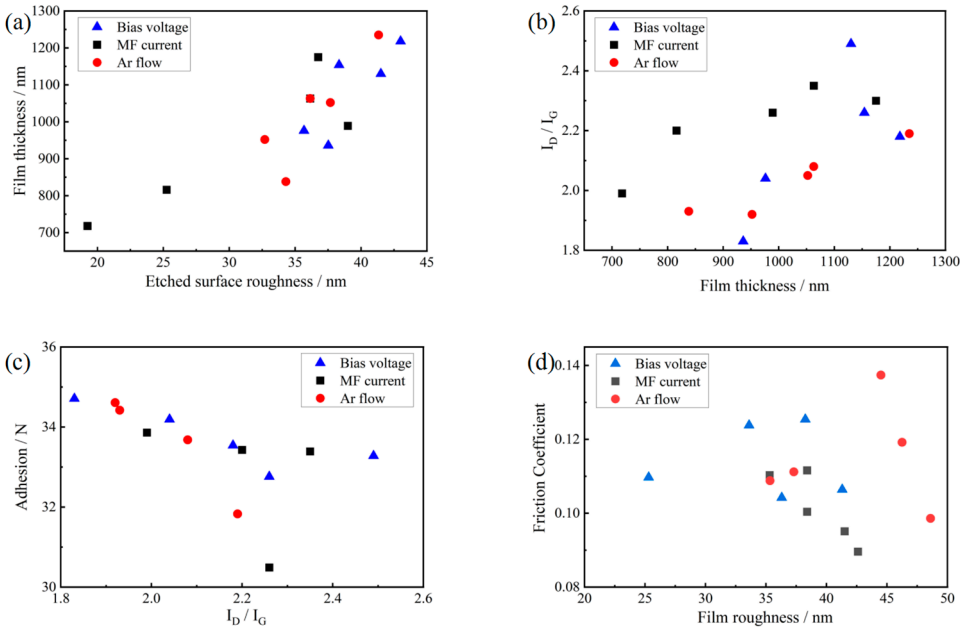


Figure 9. The influence of substrate roughness on the properties of DLC films: (**a**) film thickness related to etched surface roughness; (**b**) I_D/I_G related to film thickness; (**c**) adhesion strength related to I_D/I_G; (**d**) coefficient of friction related to film roughness.

The bonding status of C atoms in Ti-DLC films was detected through Raman spectroscopy. After Gaussian fitting, the ID/IG ratio was obtained. The overall correlation between ID/IG and film thickness is not strong. However, when comparing the three groups of samples with different etching parameters separately, it can be found that within each group, ID/IG generally increases with the increase in film thickness. This indicates that as the thickness increases, the bonding mode of C atoms in the film gradually shifts from sp^3 to sp^2 phase. The film adhesion strength measured by the scratch method shows a slow downward trend with the decrease in sp^3 hybridized bonds in the film. The lack of significant change in adhesion strength is due to the high roughness of the film. In the scratch test, film damage can easily occur due to the fracture of some peak morphologies. This is because the overall adhesion strength exhibited by the film is relatively low.

After measuring the roughness of the film, it was found that the film roughness fluctuates between 30 and 45 nm. The film roughness exhibits a random distribution characteristic, which is not related to the substrate roughness or film thickness. After rubbing the Ti-DLC film against a TC4 ball, the coefficient of friction was measured. When comparing the coefficient of friction with the film roughness, no correlation was found.

3.2.2. C/W Ratio

The main component of YG8 cemented carbide is WC grains. Taking the C/W ratio as a variable, a horizontal comparison of the typical characteristics of DLC films deposited on the etched surface is shown in Figure 10. The distribution of I_D/I_G, bonding strength, and friction coefficient of the DLC films with respect to the C/W ratio was scattered, with no

clear distribution pattern emerging. This indicates that the C/W ratio has an insignificant influence on the deposition of DLC films. Theoretically speaking, the reduction in C element on the substrate surface will leave many W atoms as dangling bonds. When depositing the DLC film, these W atoms can more easily capture carbon atoms to form bonds, thereby enhancing the bonding between the DLC film and the substrate, which can improve the adhesion strength of the film. However, in reality, during the etching process, after the W-C bonds are broken, they immediately bonded to surrounding atoms. The bonding targets could be the same W atoms or C atoms that have not been removed from the substrate or even adsorbed free Co atoms. The state of dangling bonds cannot be maintained for a long time. Therefore, when depositing the DLC film, the dangling bonds on the substrate surface had already reached a passivated state. Although the chemical activity of the surface atoms was very high after etching, the difference in the C/W ratio did not bring any other effects.

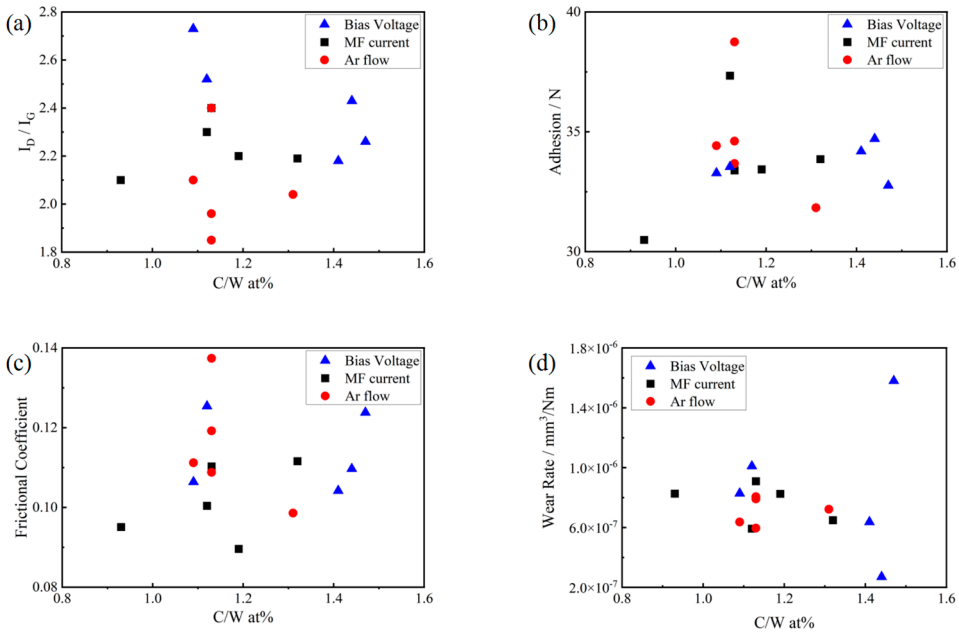


Figure 10. Ti-DLC properties with C/W ratios: (**a**) I_D/I_G; (**b**) adhesion strength; (**c**) friction coefficient; (**d**) wear rate.

Near the C/W ratio of 1.12, the properties of the DLC films exhibited a trend of vertical alignment. The C/W ratio was almost the same, which meant that this variable could be disregarded. The differences in film properties at this time indicated that there must have been other factors affecting the films.

3.2.3. Co Content

Eight samples with C/W ratios ranging from 1.09 to 1.13 were selected for further comparative analysis. A specific factor that was identified was the content of Co element. Co, which is the primary component in cemented carbide besides WC, acts as a binder for WC grains, and enhances toughness. Some studies have suggested that Co in the substrate during DLC film deposition can increase the sp^2 phase and inhibit the formation of sp^3 hybridized bonds [28,29]. The main reason is that the aggregated Co has a solubilizing effect on C atoms. When the temperature decreases, C atoms will be precipitated in the form of graphite phase. It directly leads to a reduction in the sp^3 hybridized bonds and a decrease in the adhesion between the film and the substrate [30,31].

The correlation between the relevant properties of these eight samples and the Co content on the etched surface was studied as shown in Figure 11. As the Co content

gradually increased, the I_D/I_G ratio in the DLC films showed a decreasing trend, from 2.73 to 1.85, indicating an increase in the proportion of sp^3 hybridized bonds in the films. This finding differs from existing research results. The biggest difference lay in the temperature and the form in which Co exists. The temperature for both etching treatment and Ti-DLC film deposition was lower than 150 °C, at which temperature the Co element would not diffuse in large quantities. Due to the strong etching effect of Ti ion etching treatment, the Co element in the substrate surface layer was largely removed and hardly aggregated. The remaining Co elements were mainly present in the intergranular spaces and the subsurface layer. In the etching process, most of the energy of Ti ions was conducted into the substrate. Some Ti ions moved along the substrate surface. Due to the large roughness, the energy released by the blocked Ti ions could be transferred into the gaps. Therefore, Co could obtain higher diffusion energy. In this situation, the Co content in the substrate surface layer was very low, while the Co content in the sub-surface layer had a higher diffusion energy. Co diffused to the substrate surface in a small amount of free state, rather than in the aggregated state originally present in the cemented carbide. The effect of free-state Co at the film–substrate interface on the thin film can be compared to that of Cu. When doping DLC films with extremely low amounts of Cu, the concentration of Cu was not sufficient to form nanocrystals, and it was also difficult to form C-Cu bonds. Cu atoms were embedded in the network structure of C atoms in a free state, which may raise the ratio of sp^3 bonds in DLC films [32]. The free-state Co atoms were also embedded in the network structure of the DLC film. The Co atoms can alleviate the disorder of C-C bonds and reduce bond angle distortion. It helped to mitigate the accumulation of internal stress in the thin film. Although it would cause the transformation from sp^3 bonds to sp^2 bonds, the negative effect was hard to propagate into the interior of the film, since Co only existed at the surface layer of the substrate. Therefore, Co at the interface played a role in mitigating stress concentration, thereby reducing internal stress and increasing the content of sp^3 bonds. Moreover, Co can act as a heterogeneous nucleation site, which is conducive to the growth of DLC films.

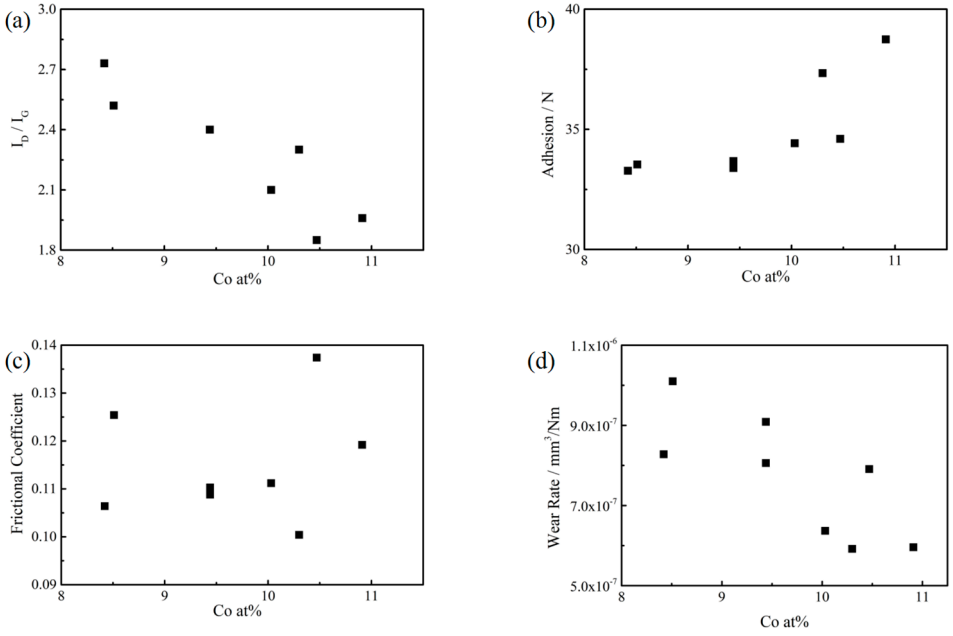


Figure 11. Ti-DLC properties with Co content: (**a**) I_D/I_G; (**b**) adhesion strength; (**c**) friction coefficient; (**d**) wear rate.

The increase in Co content improved the bonding strength of the DLC films, with the bonding force increasing from 33.28 N to 38.75 N. There was a clear correlation between

the change in bonding force and the I_D/I_G ratio, confirming that sp^3 hybridized bonds supports bonding strength. There was no clear correlation between the friction coefficient of the DLC films and Co content. However, the wear rate decreased as Co content increased, from 1.01×10^{-6} $mm^3/(N \cdot m)$ to 5.921×10^{-7} $mm^3/(N \cdot m)$, enhancing the wear resistance of the films. The reduction in wear rate was not directly related to the Co content. Instead, it was because both the adhesion strength and the sp^3 hybridized bonds of the film increased when the Co content increased. Thanks to the reinforcement of the internal structure of the film, the wear resistance was enhanced. The coefficient of friction had no clear correlation with film roughness, C/W ratio, or Co content. The variability of the coefficient of friction was related to many factors. Since the overall content of sp3 hybridized bonds was low, the strength of the film was not high. Therefore, during the initial running-in stage of friction, the film would experience rapid, minor wear. For film surfaces with high roughness, wear debris generated during wear would enter the wear track and fill the pits on the film surface. Thus, during the stable friction stage, the correlation between the film's coefficient of friction and roughness was very small.

4. Conclusions

This paper explored the influence of Ti ion etching pretreatment process on the surface properties of cemented carbide, as well as the mechanism by which the changes in surface characteristics affect the properties of Ti-DLC coatings, revealing the correlation between key process parameters and interfacial properties.

The substrate negative bias determined the energy of Ti ions. An increase in bias was accompanied by an increase in etching depth and roughness. At a voltage of −1400 V, the etching depth could reach 750 nm. The medium-frequency current controlled the excitation and density of Ti ions. Increasing the density of Ti ions had a limited effect on the etching rate, but it could enhance the lateral etching of Ti ions on the grains and increase roughness. The Ar flow rate controlled the movement and sputtering of ions on the substrate surface. It promoted the diffusion of deep-layer Co elements. A Ti-DLC film with good adhesion strength and tribological properties could be obtained under the process parameters of a bias voltage of −1100 V, medium-frequency current of 5.0 A, and Ar flow rate of 125 sccm.

The increase in substrate surface roughness could provide more nucleation sites for C atoms, thereby increasing the deposition rate of DLC films. However, excessive roughness could also lead to stress concentration, weakening the adhesion strength. The decrease in the surface C/W ratio could not provide more W atoms to bond with C atoms. This had little effect on the film. The diffusion of sub-surface Co elements could increase the proportion of sp^3 hybridized bonds by relieving stress concentration. This played a positive role in enhancing the adhesion strength and wear resistance of the film.

Author Contributions: Conceptualization, C.L.; methodology, C.L.; software, C.L.; validation, C.L.; formal analysis, C.L. and L.H.; investigation, C.L. and L.H.; resources, C.L.; data curation, C.L.; writing—original draft preparation, C.L.; writing—review and editing, L.H.; visualization, L.H.; supervision, L.H.; project administration, J.C.; funding acquisition, J.C. All authors have read and agreed to the published version of the manuscript.

Funding: This research was funded by Natural Science Foundation of the Jiangsu Higher Education Institutions (grant number: 24KJB460024).

Data Availability Statement: The raw data supporting the conclusions of this article will be made available by the authors on request.

Conflicts of Interest: The authors declare no conflict of interest.

References

1. Su, Y.; Huang, W.; Cai, L.; Gong, X.; Zhang, T.; Hu, R.; Zhang, P.; Ruan, H. Microstructural evolution and tribology of Mo-doped diamond like carbon nanocomposite film. *Tribol. Int.* **2022**, *174*, 107774.
2. Peng, Y.; Peng, J.; Wang, Z.; Xiao, Y.; Qiu, X. Diamond-like Carbon Coatings in the Biomedical Field: Properties, Applications and Future Development. *Coatings* **2022**, *12*, 1088. [CrossRef]
3. Wei, C.; Pan, W.; Hung, M. The effects of substrate roughness and associated surface properties on the biocompatibility of diamond-like carbon films. *Surf. Coat. Technol.* **2013**, *224*, 8–17.
4. Tzeng, S.; Wu, Y.; Hsu, J. The effects of plasma pre-treatment and post-treatment on diamond-like carbon films synthesized by RF plasma enhanced chemical vapor deposition. *Vacuum* **2008**, *83*, 618–621. [CrossRef]
5. Khan, S.A.; Oliveira, J.; Ferreira, F.; Emami, N.; Ramalho, A. Surface Roughness Influence on Tribological Behavior of HiPIMS DLC Coatings. *Tribol. Trans.* **2023**, *66*, 565–575.
6. Jacob, A.; Gangopadhyay, S.; Satapathy, A.; Mantry, S.; Jha, B.B. Influences of micro-blasting as surface treatment technique on properties and performance of AlTiN coated tools. *J. Manuf. Process.* **2017**, *29*, 407–418.
7. Ozeki, K.; Masuzawa, T.; Hirakuri, K.K. The wear properties and adhesion strength of the diamond-like carbon film coated on SUS, Ti and Ni-Ti with plasma pre-treatment. *Biomed. Mater. Eng.* **2010**, *20*, 21–35.
8. Lee, J.A.; Lin, C.R.; Pan, P.C.; Liu, C.W.; Sun, A.Y. Dramatically enhanced mechanical properties of diamond-like carbon films on polymer substrate for flexible display devices via argon plasma pretreatment. *Chem. Phys.* **2020**, *529*, 110551.
9. Nakao, S.; Kimura, T.; Suyama, T.; Azuma, K. Conductive diamond-like carbon films prepared by high power pulsed magnetron sputtering with bipolar type plasma based ion implantation system. *Diam. Relat. Mater.* **2017**, *77*, 122–130. [CrossRef]
10. Liu, L.; Wang, T.; Huang, J.; He, Z.; Yi, Y.; Du, K. Diamond-like carbon thin films with high density and low internal stress deposited by coupling DC/RF magnetron sputtering. *Diam. Relat. Mater.* **2016**, *70*, 151–158.
11. Jiang, J.; Huang, H.; Wang, Q.; Zhu, W.; Hao, J.; Liu, W. Comparative study on structure and properties of titanium/silicon mono- and co-doped amorphous carbon films deposited by mid-frequency magnetron sputtering. *Surf. Interface Anal.* **2014**, *46*, 139–144. [CrossRef]
12. Ponce, S.; Calderon, N.Z.; Ampuero, J.L.; La Rosa-Toro, A.; Talledo, A.; Gacitúa, W.; Pujada, B.R. Influence of the substrate bias on the stress in Ti-DLC films deposited by dc magnetron sputtering. Journal of physics. *Conf. Ser.* **2020**, *1558*, 12009. [CrossRef]
13. Wu, Y.; Shi, B.; Liu, Y.; Wang, L.; Gao, J.; Shen, Y.; Wang, Y.; Ma, Y.; Yu, S. Design of Ta gradient layer to improve adhesion strength between Cu substrate and DLC film. *Vacuum* **2022**, *203*, 111221. [CrossRef]
14. Kashyap, V.; Ramkumar, P. DLC coating over pre-oxidized and textured Ti6Al4V for superior adhesion and tribo-performance of hip implant. *Surf. Coat. Technol.* **2022**, *440*, 128492. [CrossRef]
15. Wang, X.; Sui, X.; Zhang, S.; Yan, M.; Lu, Y.; Hao, J.; Liu, W. Impacts of the a-Si:H interlayer nanostructure on the adhesion of the thick DLC coatings prepared by PECVD. *Appl. Surf. Sci.* **2021**, *565*, 150539. [CrossRef]
16. Kubart, T.; Fernandes, D.F.; Nyberg, T. On the description of metal ion return in reactive high power impulse magnetron sputtering. *Surf. Coat. Technol.* **2021**, *418*, 127234. [CrossRef]
17. Guo, C.Q.; Li, H.Q.; Peng, Y.L.; Dai, M.J.; Lin, S.S.; Shi, Q.; Wei, C.B. Residual stress and tribological behavior of hydrogen-free Al-DLC films prepared by HiPIMS under different bias voltages. *Surf. Coat. Technol.* **2022**, *445*, 128713. [CrossRef]
18. Nakao, S.; Yukimura, K.; Nakano, S.; Ogiso, H. DLC Coating by HiPIMS: The Influence of Substrate Bias Voltage. *IEEE Trans. Plasma Sci.* **2013**, *41*, 1819–1829. [CrossRef]
19. Wasy, A.; Balakrishnan, G.; Lee, S.H.; Kim, J.K.; Kim, D.G.; Kim, T.G.; Song, J.I. Argon plasma treatment on metal substrates and effects on diamond-like carbon (DLC) coating properties. *Cryst. Res. Technol.* **2014**, *49*, 55–62. [CrossRef]
20. Nguyen, T.; Ulrich, S.; Bsul, J.; Beauvais, S.; Burger, W.; Albers, A.; Stüber, M.; Ye, J. Influence of argon gas pressure and target power on magnetron plasma parameters. *Diam. Relat. Mater.* **2009**, *18*, 995–998. [CrossRef]
21. Bonu, V.; Srinivas, G.; Kumar, V.P.; Joseph, A.; Narayana, C.; Barshilia, H.C. Temperature dependent erosion and Raman analyses of arc-deposited H free thick DLC coating on Cr/CrN coated plasma nitrided steel. *Surf. Coat. Technol.* **2022**, *436*, 128308. [CrossRef]
22. Fu, Z.Q.; Wang, C.B.; Yue, W.; Peng, Z.J.; Lin, S.S.; Dai, M.J. Influence of Vacuum Cathodic Arc Etching on Structure and Properties of W-Doped DLC Films. *Adv. Mater. Res.* **2013**, *787*, 296–300. [CrossRef]
23. Tillmann, W.; Dias, N.F.; Stangier, D.; Maus-Friedrichs, W.; Gustus, R.; Thomann, C.A.; Moldenhauer, H.; Debus, J. Improved adhesion of a-C and a-C:H films with a CrC interlayer on 16MnCr5 by HiPIMS-pretreatment. *Surf. Coat. Technol.* **2019**, *375*, 877–887.
24. Santiago, J.A.; Fernández-Martínez, I.; Wennberg, A.; Molina-Aldareguia, J.M.; Castillo-Rodríguez, M.; Rojas, T.C.; Sánchez-López, J.C.; González, M.U.; García-Martín, J.M.; Li, H.; et al. Adhesion enhancement of DLC hard coatings by HiPIMS metal ion etching pretreatment. *Surf. Coat. Technol.* **2018**, *349*, 787–796.
25. Peng, B.; Xu, Y.X.; Du, J.W.; Chen, L.; Kim, K.H.; Wang, Q. Influence of preliminary metal-ion etching on the topography and mechanical behavior of TiAlN coatings on cemented carbides. *Surf. Coat. Technol.* **2022**, *432*, 128040.

26. Li, C.; Huang, L.; Yuan, J.; Zhou, D. The influence of Ti plasma etching pre-treatment on mechanical properties of DLC film on cemented carbide. *Surf. Interface Anal.* **2022**, *54*, 477–486. [CrossRef]
27. Ward, L.; Junge, F.; Lampka, A.; Dobbertin, M.; Mewes, C.; Wienecke, M. The Effect of Bias Voltage and Gas Pressure on the Structure, Adhesion and Wear Behavior of Diamond Like Carbon (DLC) Coatings With Si Interlayers. *Coatings* **2014**, *4*, 214–230. [CrossRef]
28. Liu, K.; Wang, Z.; Yin, Z.; Cao, L.; Yuan, J. Effect of Co content on microstructure and mechanical properties of ultrafine grained WC-Co cemented carbide sintered by spark plasma sintering. *Ceram. Int.* **2018**, *44*, 18711–18718.
29. Zhang, D.; Shen, B.; Sun, F. Study on tribological behavior and cutting performance of CVD diamond and DLC films on Co-cemented tungsten carbide substrates. *Appl. Surf. Sci.* **2010**, *256*, 2479–2489.
30. Li, B.; Zhang, Y.; Wu, Z.; Qin, Z.; Ji, H.; Liu, X.; Li, B.; Hu, W. Magnetic properties and corrosion resistance of Co-DLC nanocomposite films with different cobalt contents. *Diam. Relat. Mater.* **2021**, *117*, 108477.
31. Tang, Y.; Li, Y.S.; Zhang, C.Z.; Wang, J.; Yang, Q.; Hirose, A. Synthesis of cobalt/diamond-like carbon thin films by biased target ion beam deposition. *Diam. Relat. Mater.* **2011**, *20*, 538–541.
32. Guo, P.; Sun, L.; Li, X.; Xu, S.; Ke, P.; Wang, A. Structural properties and surface wettability of Cu-containing diamond-like carbon films prepared by a hybrid linear ion beam deposition technique. *Thin Solid Films* **2015**, *584*, 289–293.

Disclaimer/Publisher's Note: The statements, opinions and data contained in all publications are solely those of the individual author(s) and contributor(s) and not of MDPI and/or the editor(s). MDPI and/or the editor(s) disclaim responsibility for any injury to people or property resulting from any ideas, methods, instructions or products referred to in the content.